Method of LANTCET for cancer diagnostics and treatment at cell level

E. Hleb*, I. Zastinskaya**, I. Ilyukova**, I. Koneva**, A. Uss***, I. Semenenya****, J. Hafner*****, E. Hanna ******, J. Myers******, S. Zhdanok*, and D. Lapotko*

*A. V. Lykov Heat & Mass Transfer Institute, 15 P. Brovka St., Minsk, 220072, Belarus, ld@hmti.ac.by
**Belarusian Center of Hygiene, 8 Akademicheskay St., Minsk, 220072, Belarus
***Belarusian Center of Hematology & Transplantology, Semashko St., Minsk, 220089, Belarus
****Ministry of Healthcare of Belarus, 39 Miasnikov St., Minsk, 220048, Belarus
*****Rice University, 6100 Main St. Houston, TX 77005, USA
******The University of Texas M.D. Anderson Cancer Center, 1515 Holcombe Blvd, Houston, TX 7700A, USA

ABSTRACT

We have developed the method of LANTCET (laser-activated nano-thermolysis as a cell elimination technology) for selective detection and destruction of individual tumor cells by generating intracellular photothermal bubbles around the clusters of gold nanoparticles. Bare nanoparticles and their conjugates with the C225 tumor-specific monoclonal antibodies were applied in vitro to the C225-positive squamous carcinoma cells and in vivo to an experimental tumor in a rat to form intracellular clusters of nanoparticles (NP). Single 10 ns laser pulses generated intracellular photothermal micro-bubbles (PTB) at a near-infrared and visible wavelengths. The cells with the clusters have yielded almost 100-fold decrease in laser fluence thresholds for bubble generation and cell damage relatively to those for the cells without clusters. Cell damage had a mechanical origin and single cell selectivity. Three LANTCET processes (cell detection, damage, and optical guidance) were realized as a microsecond sequence and with the one device.

Keywords: laser, nanoparticle, bubble, scattering, cancer

1 INTRODUCTION

Gold nanoparticles (NPs) that absorb strongly in visible and near-infrared optical range hold great potential as diagnostic and therapeutic agents that are also non-toxic to normal organs. We have recently introduced the method of laser-activated nano-thermolysis as a cell elimination technology (LANTCET) [1-5], based on mechanical, but not thermal destruction of individual target cells with laser pulses. This method utilizes vapor microbubbles generated by short laser pulses around superheated NPs. In our previous studies we have demonstrated the cell targeting protocol that resulted in the formation of NP clusters capable of significantly improving the efficacy, selectivity and safety of laser-activated nano-thermolysis, as compared to single NPs. The actual formation of the NP clusters in cells was noticed in many experiments, but the clusters were not considered as specific diagnostic or therapeutic agents. The main purpose of our work was to perform feasibility study of the method that is aimed at tumor detection, treatment and the guidance of the treatment at cell level. To evaluate the potential of the LANTCET method for the treatment of solid superficial tumors we have experimentally studied several combinations of biological models, gold NP types and laser wavelengths.

2 MATERIALS AND METHODS

2.1 Method of laser of laser-activated nano-thermolysis as cell elimination technology (LANTCET)

The method for selective elimination of target tumor cells includes the two main steps: (a) intravenous or topical application of gold NP conjugates to provide their selective accumulation in target tumor cells by using tumor-specific monoclonal antibodies (MAB) or other vectors conjugated to NP, resulting in selective formation of NP clusters in the target tumor cells, and (b) selective mechanical (non-thermal) destruction of tumor cells by photothermal (PT) vapor micro-bubbles generated by short laser pulses around NP clusters in individual target cells.

High selectivity of NP clusters formations in the target tumor cells in comparison with the accumulation of single NPs in any cells is provided by two biological mechanisms. First, NP-MAB conjugates are selectively coupled with the matching tumor-specific receptors (such as epidermal growth factor receptor -EGFR) at cell membrane. Secondly, during receptor-mediated endocytosis the NPs are internalized and concentrated into the clusters in endosomal compartments. Cluster formation was performed *in vitro* by incubating the cells with NPs at the temperature at 37°C and during 30 - 60 minutes to stimulate internalization of NPs through endocytosis. At the end of the incubation

procedure large NP clusters are formed only in those cells with high initial levels of membrane-bounded NPs, i.e. the target cells, as we have shown earlier.

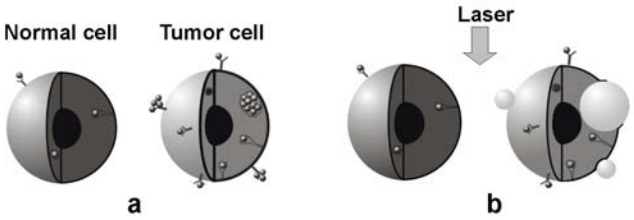

Figure 1: Block diagram of the experimental protocol for LANTCET: (a) clusterization of NP, (b) laser-induced vapor bubbles and cell damage.

We suggest that the main cell damaging process not hyperthermia but laser-induced bubbles, generated selectively around the clusters of NP. Besides a cell damage function, the NP clusters and the PT bubbles have good optical scattering coefficients and therefore can be used (a) for optical detection of the target cell through optical scattering from NP clusters and (b) for the guidance of the cell damage through optical scattering detection of the PT bubbles with additional probe laser beam of low intensity. Thus the PT bubbles can be used as the cell damaging agents and as the optical markers for real time optical guidance of the tumor treatment. So the LANTCET (Fig. 1) includes four major stages: (a) formation of cell-specific NP clusters; (b) optical detection of tumor cells (with clusters of NPs) using NP cluster-specific optical scattering, (c) selective mechanical damage of individual tumor cells by pulsed laser-induced PT bubbles selectively generated around NP clusters in individual target cells, and (d) real-time optical guidance of tumor cell damage by detecting (imaging) of PT bubble-specific scattering optical signal.

2.2 Experimental model

Individual cells. Solid tumor cells were prepared as the monolayers of living EGF-positive carcinoma cells (Hep-2C and A549) that were grown into standard 9-mm culture wells to 70% confluence. As the normal cells we used human red blood cells and lymphocytes. We also used the tumor cells, which were not treated with NPs, for control. All cells were incubated with NPs for 30 min at 37°C. Several different NPs were used: gold spheres (NSP), gold nanorods (NRs) and gold nanoshells (NS) (bare and conjugated with the MAB C225). Individual cells were irradiated with single laser pulse at 532 nm, which is close to the peak of maximum optical NSP absorbance, or at 760 nm, which is close to the peak of maximum optical absorbance of NS and NR and their clusters. The damage to the cell membrane was verified by staining the cells after their exposure to laser pulse with the Trypan Blue dye at the concentration of 0.4% .

Animal model. Rats were used to grow experimental polymorphic Sarcoma 1 to the diameter of 5-6 mm. The animals were anesthetized prior to the LANTCET treatment. The skin layer was removed at the tumor site to provide better access of NPs to the tumor. Gold spherical 30 nm particles (NSP) conjugated to goat anti-mouse IgG were applied topically on the tumor surface and left for 40 min in room temperature. A single 532-nm laser pulse (maximum of light absorbance by NSP), 10 ns duration, fluence of 0.75 J/cm^2 and 3-mm diameter was directed to the central area of the tumor. The degree of tumor necrosis was measured according to the uptake of Evans Blue by the tumor tissue with a standard extravasation method.

3 RESULTS

We have studied an uptake of gold NR by individual C225-positive cells (Hep-2C) with optical scattering microscopy. The accumulation of NSP in the cells was studied by us in detail before and in this work we have focused on the study of NR and of NS interactions with the cells. Optical scattering imaging yielded localized signals in the Hep-2C cells after their incubation with the NR-C225. Observed high accumulation of NR was provided by interaction of EGFR specific MAB – C225 – with EGF receptors that are overexpressed by these cells. The amplitudes of optical scattering signals for Hep-2C cells were found to be 547.3±195.0 counts for intact control cells and 2766.7±907.4 counts for NR-treated cells as population-averaged values. Obtained images of the cells revealed the two common features: NR-related optical signals (a) were detected in 90-95% of treated cells and (b) spatial distribution of NR-related signals within the cell was highly heterogeneous with apparent local peaks with spatial dimensions being less than 1 μm, and the peak amplitude values up to 10,000-12,000 counts. Discovered local signals are significantly stronger than scattering signals from single NRs. Therefore cellular sources of the detected signals can be attributed as NR clusters. Providing the small size of NRs we can assume that they penetrated through outer cellular membrane via the mechanism of endocytosis and then were concentrated into the clusters. Such mechanism of accumulation and clusterization of gold NSP was already proved by us earlier for leukemia cells. The studies of optical scattering has shown that only NP clusters may provide sufficient signal-to-noise ratio for reliable detection of specific tumor cells.

We have experimentally verified for many types of culture and human cells that laser-induced PT vapor bubbles destroy the cell and this damage mechanism requires only a single laser pulse. We have also found out that the bigger cluster size, the lower laser fluence threshold of bubble generation. The PT bubble may reach the diameter of several micrometers with the lifetime being up to several microseconds. Applying a single pulse with the energy (fluence) at the minimal level provides bubble

generation only around the biggest NP clusters (>200 nm) and does not induce any bubbles around smaller clusters or around single NPs (which have a higher threshold for bubble generation). Such laser fluence level provides high selectivity of cell damage: no PT bubbles can be generated in normal cells even if they accumulated some NPs.

Generation of PT bubbles in cells was studied *in vitro* for several types of gold NPs. In this study we have applied the photothermal (PT) microscope previously developed by us for generating and detecting PT bubbles in individual cells. Pump and probe laser beams were focused on a specific cell positioned manually with microscope stage into the center of laser beams. Each cell was exposed to a single pump pulse (10 ns). During the laser pulse the two optical signals were obtained simultaneously – the time response (with continuous probe laser 633 nm) from the whole cell (not show) and time-resolved (with pulse probe laser with 20 ns delay to pump pulse) images to visualize short-living PT bubbles induced by the pump laser pulse in this cell (Fig. 2b). It allowed us to detect and to measure the PT bubbles in the cell. The optical images of each cell were obtained before (Fig. 2a) and 2-5 seconds after its irradiation with a pump laser pulse (Fig. 2c). This allowed us to check morphological integrity of the cell after the laser pulse. A population of 100 cells was studied under identical irradiation conditions within approx. 10-15 min. PT bubbles were identified according to the time responses of negative and symmetrical shape that is specific for PT bubbles (not show) and they were also detected in time-resolved images. Bubble-specific image is shown at Fig. 2c. It was obtained for individual A549 and Hep-2C cells after their 30 min incubation with NS-C225 conjugates. Peripheral location of the bubble-specific signals in the time-resolved image of tumor cell shows that the bubbles were generated in the cytoplasm and presumably not in the nuclei.

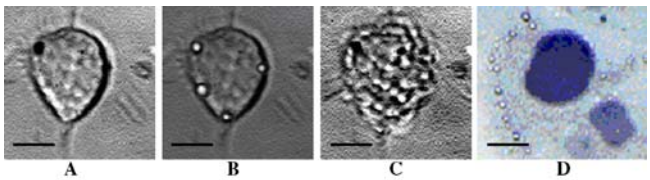

Figure 2: Optical microscopic images of A549 (C225-positive) cell with the clusters of NSs before (a) and 5 s after (c) exposure to a single laser pulse (10 ns, 750 nm, 0.7J/cm^2), (b) the image of PT bubbles in this cell, (d) similar cell stained with Trypan Blue after the treatment with NPs and with laser pulse. Scale bar is 10 μm.

As the laser fluence increased, the PT bubble generation probability (*PRB)* values gradually increased from 0 to 1 and the monotonous character of the *PRB*(ε) dependence was found to be typical for all studied cells and NPs. Obtained dependences of *PRB*(ε) (not shown) were used to determine laser fluence thresholds for PT bubble generation (Table 1). We have found that PT bubble threshold levels for the C225-positive cells were the lowest when NS-C225 conjugates were applied. Incubation of the same cells with bare, non-conjugated NSs resulted in 22 times higher threshold which coincided with that, measured for the water suspension of non-aggregated NSs. Additionally we have incubated the C225-negative cells – lymphocytes - with NS-C225 conjugates. Corresponding PT bubble generation threshold in this case was found to be very close to that obtained for the water suspension of non-aggregated NSs (Table 1). This means that single NSs might occasionally get into non-target cells though they did not form NP clusters. The PT bubble generation thresholds for the different intact tumor cells that were not incubated with NSs and were used as additional control were significantly higher (Table 1). The difference between the PT bubble generation thresholds for the intact cells and those treated with gold NSs reached almost 2 orders of magnitude.

NP type and cell incubation conditions	Lymp-hocytes	Red blood cells	Hep-2C	Single NPs in water
NS (bare)	-	-	11.0±2.5	-
NS-C225 (conjugate)	12.0±1.2	-	0.5±0.1	11.0±1.7
No particles – intact cells	> 40	> 50	> 40	-

Table 1: Laser fluence thresholds (J/cm^2) for generation of PT bubbles (laser pulse 750 nm, 10 ns) in normal and tumor cells.

The analysis of the optical images of individual cells after pump laser pulse accompanied by PT bubbles in the cells (Fig. 2a,c) and later Trypan Blue staining (Fig. 2d) has revealed that cellular membranes were damaged each time when the bubbles were generated in the cell. Significant cell damage (*LD*) was found among the both types of the cells at the laser fluence level of 0.7 J/cm^2: for A549 cells *LD* was 0.73±0.1. For Hep-2 cells *LD* was found to be 0.93±0.04 (the level 1.0 corresponds to the damage of 100% of the cells). The difference in the laser damage levels of Hep-2C and A549 cells is not significant and allows to conclude that the mechanism of cell damage is rather universal providing that the cells form the clusters of NPs. Correlation of the *LD* and *PRB* allows to consider PT bubbles for real-time optical guidance of the cell damage process. So we may correlate the cell death to the bubble generation. Earlier we have thoroughly studied this kind of correlation for several types of various leukemia cell. We have found that the detection of the bubbles with the lifetime above 100 ns always resulted in cell damage. This means that a single laser pulse accompanied by PT bubble has caused cell death. Therefore cell death can be optically detected according to the bubble-specific signal–image or response. This can be done in real time and eliminates the need for additional diagnostic procedures. This feature of

the bubbles allow us to use them for optical guidance of the therapy.

We have used an animal model for further evaluation of feasibility of the LANTCET. Rats were implanted with sarcoma cells intra- and sub-dermal to yield tumors 5-6 mm in diameter and were then anesthetized prior to topical application of the nanoparticles (Fig. 3a). Figure 3 shows vertical cross sections of the two tumor slices: treated with NPs and with a single laser pulse (Fig. 3c) and treated only with the identical laser pulse (Fig. 3d). The LANTCET-treated tumor showed non-viable (white) area with the diameter close to the laser beam diameter (3-4 mm) and the depth of 1-2 mm that may indicate diffusion depth of NPs into the tumor.

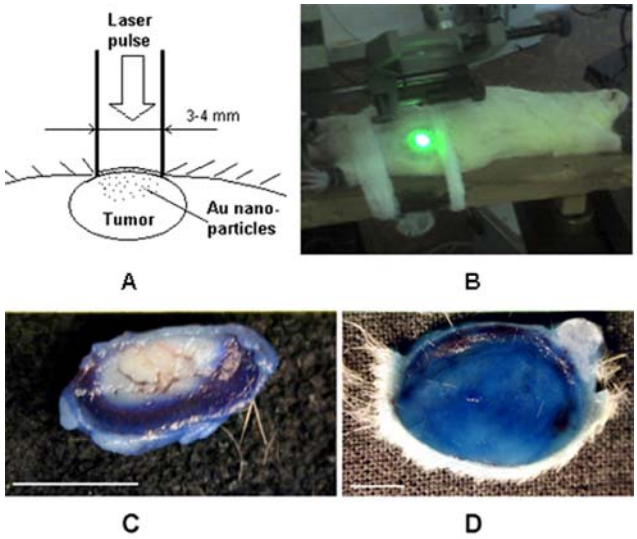

Figure 3: Scheme of the LANTCET treatment of the tumor in rat (a) and experimental set up (b), vertical cross section (slice) of the tumor: (c) treated with nanoparticles and a single laser pulse, (d) treated with laser; tumor slices were stained with Evans Blue after laser treatment and extraction from the animals (blue – intact area, white – damaged area); scale bar is 5 mm.

The tumor that underwent laser treatment without pretreatment with NPs showed no signs of any damage and appeared to be viable. The conditions of NP-cell interaction (physiological temperature and 40-minute incubation time) were sufficient to provide the formation of NP clusters in tumor cells as previous *in vitro* experiments have shown. The level of laser fluence applied during *in vitro* experiments turned to be too low for the PT bubble generation around single NPs but, on the other hand, was sufficient for PT bubble generation in the cells having NP clusters. Therefore we may assume that the main mechanism of tumor damage in the animal model is also associated with cluster-bubble effect. This implies superficial tumor as the most probable therapeutic application of the LANTCET in a surface scan mode.

4 CONCLUSION

Described above method LANTCET allows to use one micro-device for three clinically relevant steps:

- detection of target cells with optical scattering from NP clusters ;
- selective mechanical damage of individual tumor cells through the generation of intracellular PT bubbles;
- optical guidance of cell damage based on the detection of bubble-specific optical signal or image.

Comparing LANTCET with other laser methods for cell damage (based on photo-activated chemical reactions or photothermal effects not confined by individual cells) we may point out several potential advantages, which would provide better clinical efficacy, safety and applicability of laser nano-technologies:

- non-toxic agents (gold NP are non-toxic in comparison with dyes and drugs);
- mechanical, non-thermal mechanism of cell damage that can be localized within a specific cell;
- minimal amount of NPs is required to form NP cluster;
- NP clusters instead of single NPs greatly improve the selectivity of cell killing and also allow to decrease laser pulse energy below the damage level to normal tissues;
- optical properties of PT bubbles allow real time optical guidance.

REFERENCES

[1] D. Lapotko, E. Lukianova, M. Potapnev, O. Aleinikova, A. Oraevsky, "Method of laser activated nanothermolysis for elimination of tumor cells," Cancer Lett., 239, 36-45, 2006.

[2] D. Lapotko, E. Lukianova, A. Oraevsky, "Selective laser nano-thermolysis of human leukemia cells with microbubbles generated around clusters of gold nanoparticles," Lasers Surg. Med., 38, 631-642, 2006.

[3] D. Lapotko, E. Lukianova-Hleb, A. Oraevsky, "Clusterization of nanoparticles during their interaction with living cells," Nanomedicine, 2, 241–253, 2007.

[4] E. Y. Hleb, Y. Hu, R. A. Drezek, J. H. Hafner, D. O. Lapotko, Photothermal bubbles as optical scattering probes for imaging living cells," Nanomedicine, 3, 797-812, 2008.

[5] E. Y. Hleb, J. H. Hafner, J. N. Myers, E. Y. Hanna, B. C. Rostro, S. A. Zhdanok, D.O. Lapotko, "LANTCET: elimination of solid tumor cells with photothermal bubbles generated around clusters of gold nanoparticles," Nanomedicine, 3, 647-667, 2008.